

Rational Design of Multifunctional Tacrine Derivatives for the treatment of Alzheimer and Parkinson Diseases

Eugenia Dzib,¹ Luis Felipe Hernández-Ayala, and Annia Galano^{1,*}

¹ Universidad Autónoma Metropolitana, Unidad Iztapalapa, División de Ciencias Básicas e Ingeniería, Departamento de Química, Ferrocarril San Rafael Atlixco 186, Col. Leyes de Reforma 1^a Sección, Alcaldía Iztapalapa, 09130, Ciudad de México, México

Correspondence to Annia Galano (e-mail: agal@xanum.uam.mx)

Abstract

Alzheimer and Parkinson are the most common neurodegenerative diseases. Unfortunately, there is no therapy that prevents or slows their progress. The main drugs to treat Alzheimer's disease (AD) are acetylcholinesterase (AChE) and N-methyl-D-aspartate receptor (NMDAr) inhibitors, while catechol-*O*-methyltransferase (COMT) and monoamine oxidase B (MAO-B) inhibitors are used for Parkinson's disease (PD). Tacrine was the first FDA approved drug against AD. Although it was withdrawn due to its hepatotoxicity, its simple structure has made it widely used as a starting point for drug development. Herein, we present 1295 tacrine derivatives designed through the CADMA-Chem protocol. Their chemical space was sampled by selection scores based on ADME properties, toxicity, and manufacturability. A subset of five derivatives with the best drug-like behavior was chosen for further investigation. Acid-base parameters and reactivity indexes were computed for this subset to assess their role as antioxidants. Our findings showed that the neutral and cationic species of the TAC-678, TAC-698, and TAC-674 derivatives are better electron and H donors than tacrine and the reference antioxidants (trolox, tocopherol, and ascorbic acid). Furthermore,

according to molecular docking, TAC-674 and TAC-678 are the best inhibitors of AChE and COMT, and NMDAr and MAO-B, respectively. Hence, they are the most promising candidates to act as multifunctional antioxidants and neuroprotectors against AD and PD.

1. Introduction

Alzheimer disease (AD) and Parkinson disease (PD) are the most prevalent neurodegenerative disorders. In 2021, 40 million¹ and 11.8 million² people worldwide were living with AD and PD, respectively; and are projected to rise to 132 million³ and 25.2 million⁴ people, respectively, by 2050.

AD is characterized by the accumulation of extracellular amyloid- β (A β) plaques and intracellular tau neurofibrillary tangles (NFTs).^{5,6} Other cause of AD is the dramatic decrease of the acetylcholine (ACh) levels due to a decline in ACh synthesis by choline acetyltransferase (ChAT) combined with an increase in ACh degradation by acetylcholinesterase (AChE).⁶⁻⁸ Besides, overstimulation of the N-methyl-D-aspartate receptor (NMDAr) allows an excessive entry of sodium and calcium ions, resulting in excitotoxic damage to the neurons.^{6,9-11} Finally, oxidative stress (OS), caused by an imbalance between the production oxidizing species and their removal by the antioxidant defense system, contributes significantly to the progression of AD and is tightly linked to its aforesaid causes.^{6,12-15}

The key hallmarks of PD encompass the aggregation of α -synuclein (α -syn) as Lewy bodies¹⁶⁻¹⁸ and the progressive loss of dopaminergic neurons in the *substantia nigra pars compacta* (SNpc) leading to a depletion of dopamine (DA) levels. This triggers the onset of the characteristic motor symptoms of PD such as tremor, bradykinesia, stiffness, and postural instability.^{16,19} DA is a neurotransmitter essential for motor control, cognition, reward, and modulation of emotions.^{20,21} Nevertheless, current evidence suggests that its oxidation induce oxidative damage in dopaminergic neurons leading to their degeneration and death.¹⁹ DA oxidation can be spontaneous or be mediated by metal ions or enzymes, primarily by monoamine oxidase B (MAO-B) and catechol-*O*-methyltransferase (COMT).^{16,19,20} The

latter also metabolizes levodopa (L-DOPA) that is a DA precursor.²⁰ Particularly, with aging the MAO-B activity is increased in the human brain leading to a DA deficiency and a high production of H₂O₂ and toxic aldehydes.^{16,22-24}

Two types of drugs are still the mainstay of AD treatment: The AChE inhibitors donepezil, rivastigmine, and galantamine for mild and moderate stages of AD, and the NMDA receptor antagonist memantine for moderate and severe stages of AD.^{5-7,15,16} Recently, the FDA approved the anti-A β monoclonal antibodies lecanemab and donanemab for early-stage AD.²⁵ The most efficacious anti-parkinsonian drug is L-DOPA, but it has a short half-life. It can be combined with COMT inhibitors such as opicapone, entacapone, and tolcapone (only this can cross blood brain barrier), and MAO-B inhibitors such as rasagiline, selegiline, and safinamide. L-DOPA and MAO-B inhibitors are used when PD is in early stages, while COMT inhibitors are recommended for late stages.^{16,23,26-28} Unfortunately, except for lecanemab and donanemab, these drugs only relieve the symptoms, they cannot slow down or inhibit the progression of AD and PD.²⁹ Furthermore, memantine, lecanemab, and donanemab,²⁵ can lead to severe side effects. Therefore, due to the multifactorial nature of AD and PD as well as the limitations of the currently used therapies to treat these diseases, it is urgent to design multi-target small drugs that can improve therapeutic efficacy and safety.

Tacrine (9-amine-1,2,3,4-tetrahydroacridine, TAC, Scheme 1) was the first drug approved by FDA (Food and Drug Administration) to treat AD by inhibiting AChE. Tacrine acts by inhibiting AChE to prevent ACh degradation and it was used in mild-to-moderate AD. However, it was withdrawn from the market in 2013 due to its hepatotoxicity,³⁰⁻³⁴ linked to the hydroxylation at the C7 position during metabolism. Tacrine has been extensively used as an important starting point for drug development. This is due to its strong AChE binding

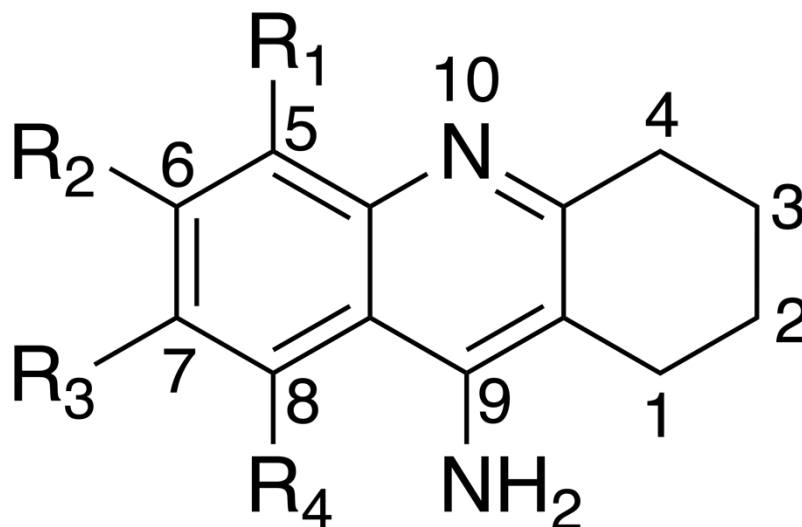
($IC_{50} = 190 \pm 1$ nM),³⁵ synthetic accessibility,³⁰ ligand efficiency,^{30,36} low molecular weight, and simple structure.^{30,36} To date, several studies have been performed to design tacrine derivatives that have shown a significant potential to inhibit the proteins AChE, NMDA receptor,^{34,37} and MAO-B.³⁴

In this work, we present a systematic and rational search of tacrine derivatives with antioxidant and neuroprotective behavior for treating Alzheimer and Parkinson diseases. This was carried out using a protocol known as CADMA-Chem (Computer-Assisted Design of Multifunctional Antioxidants based on chemical properties) which serves to identify viable compounds to treat polygenic diseases (*i.e.*, multifactorial disorders).^{38,39} To date, it has been used for neuroprotection with outstanding results.³⁸⁻⁴⁴ It were assessed the drug-like behavior, toxicity, manufacturability, antioxidant activity through electron and hydrogen atom donating capabilities, and polygenic protection by inhibiting the proteins AChE, NMDAr, COMT, and MAO-B. Consequently, the most promising candidates were proposed for future research.

2. Computational Details

2.1 Building the derivatives

Tacrine derivatives were built by inserting up to four functional groups (*i.e.*, -OH, -OCH₃, -CHO, -SH, and -COOCH₃) into the unsaturated sites of tacrine (Scheme 1, TAC-*n*, where *n* is the derivative number). These substituents were selected due to their ability to influence solubility, acid-base behavior, antiradical activity, and metal chelating capacity. The derivatives were designed with the *Smile-it* program (version 1.0) (available for download at <https://agalano.com/research/apps/desktop-apps/>).^{39,45}



Scheme 1. Tacrine (1,2,3,4-tetrahydroacridin-9-amine, R₁-R₄ = H, TAC) and the substitution sites used in this work.

2.2 Screening the chemical space

The properties of absorption, distribution, metabolism, and elimination (ADME) for all the derivatives were predicted with the *CADMA-Py*^{38,39,46} program. *CADMA-Py* estimates the ADME properties of molecular weight (MW), water/octanol partition coefficient (logP), molar refractivity (MR), number of heavy atoms (XAt), number of H-bond acceptors (HBA), number of H-bond donors (HBD), rotatable bonds (RB), and topological polar surface area (PSA). These parameters are needed to investigate if the derivatives satisfy the rules of Lipinski,⁴⁷ Ghose,⁴⁸ Egan,⁴⁹ Muegge,⁵⁰ and Veber.⁵¹

The toxicity (T) was assessed by computing the parameters of developmental toxicity (DT), Ames mutagenicity (M), and oral rat 50% lethal dose (LD₅₀) through the Consensus method, as implemented in the Toxicity Estimation Software Tool (*TEST*) software (version

5.1.2).⁵² *TEST* is based on Quantitative Structure Activity Relationships (QSARs) approaches.

The synthetic accessibility (SA) was predicted with the *Ambit-SA*⁵³ software. SA exhibits values from 0 to 100. Higher values corresponds to molecules that are easier to synthesize.

The chemical space was sampled by calculating the selection score (S^S) through the *CADMA-Py*^{38,39,46} program. S^S accounts for the bioavailability of a molecule. It is obtained from three terms that includes the ADME properties, the toxicity, and the synthetic accessibility (Text S1). The derivatives were compared against a reference set formed by compounds that have been used as neuroprotectors or are in advanced clinical phases (see below).

2.3 Reactivity descriptors

Full geometry optimizations and frequency analysis were carried out at the M05-2X⁵⁴/6-31+G(d) level. The M05-2X functional was designed for thermochemistry, kinetics, and noncovalent interactions.⁵⁴ It also has been used successfully to obtain high quality kinetic data for radical-molecule reactions in aqueous solution,^{55,56} bond-dissociation energies,⁵⁷ and pKa values.⁵⁸⁻⁶⁰ All the structures are local minima (*i.e.*, they exhibit no imaginary frequencies). Open-shell systems were studied with the unrestricted approach. The solvent (water) was mimicked through the implicit solvation model based on density (SMD).⁶¹ All the electronic structure computations were done with *Gaussian 09* Rev D.01.⁶² The energetic analysis was performed with *Eyringpy*.⁶³

Ionization energies (IE) and Bond dissociation energies (BDE) were computed using the adiabatic SCF scheme, and enthalpies, respectively. Particularly, the for the BDEs all the

most probable sites for H donation were considered (*i.e.*, the OH and the sp^3 carbons). This was done to investigate if the derivatives behave as antioxidants through the single electron transfer (SET) and hydrogen atom transfer (HAT) mechanisms.

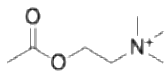
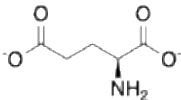
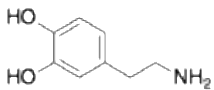
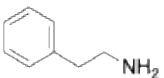
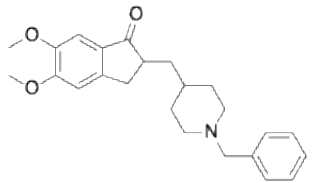
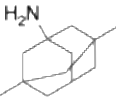
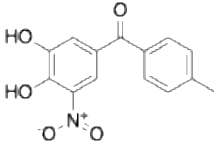
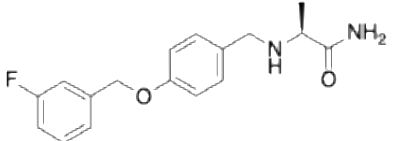
Deprotonation routes were obtained with Marvin⁶⁴ software (available at <https://playground.calculators.cxn.io/>) and were confirmed with electronic structure calculations considering all the possible deprotonation sites. The pKa values were estimated employing the fitting parameters approach. The fitted parameters (m and C_0) used are the ones for phenols (0.313, -80.020) and amines (0.475 and -124.072).⁵⁸

2.4 Molecular docking

The structures of the proteins, co-crystallized with well-known neuroprotectors, were obtained from the Protein Data Bank.⁶⁵ Their data are summarized in Table 1. The AChE misplaced loop sections (256-261 and 493-496 residues) were fixed with Modeller.⁶⁶ The energy was minimized with Swiss-PDB Viewer 4.1.⁶⁷ The proteins were prepared by eliminating water molecules, inhibitors, and species of non-interest with AutoDockTools4.⁶⁸ The atomic charges of the natural substrates, inhibitors, and ligands (*i.e.*, tacrine derivatives) were computed using the NBO protocol at the M05-2X⁵⁴/6-31+G(d) level with *Gaussian 09* Rev D.01.⁶² Molecular docking was carried out with Autodock Vina 1.2.7 software.^{69,70} A gradient optimization algorithm was used for the active site that was centered at $x = -16.30$, $y = -43.83$, and $z = 30.17$ with a grid size of $21 \times 21 \times 21$ Å for AChE; $x = 166.14$, $y = 174.34$, and $z = 216.82$ with a grid size of $15 \times 15 \times 15$ Å for NMDAr; $x = -10.49$, $y = 40.60$, and $z = 61.64$ Å with a grid size of $15 \times 15 \times 15$ Å for COMT; $x = 51.81$, $y = 156.34$, and $z = 28.15$ with a grid size of $15 \times 15 \times 15$ Å for MAO-B. The docking score (*i.e.*, the binding energy, ΔG_B) was estimated for each protein-ligand complex. This energy was weighted (ΔG_B^W , Text

S1) with the molar fractions of the relevant acid-base species (*i.e.*, with a molar fraction ≥ 1.0 %) at pH = 7.4. The best-docked pose of the most stable protein-ligand complex was analyzed and drawn with Discovery Studio.⁷¹ Redocking was performed with *Chimera* 1.17.3.⁷² The RMSD values and the binding energies for the complexes AChE-donepezil, NMDAr-memantine, COMT-tolcapone, and MAO-B-safinamide, were 2.8, 0.6, 1.6, and 1.8 Å; and -12.0, -5.8, -7.6, and -10.0 kcal mol⁻¹, respectively. They agree well with the observed values of IC₅₀, Ki, and . Therefore, our docking methodology is reliable.

Table 1. Data of the proteins used in the molecular docking.

	AChE	NMDAr	COMT	MAO-B
PDB ID	4EY7 ⁷³	7SAD ⁷⁴	3S68 ⁷⁵	2V5Z ⁷⁶
Substrate				
	Acetylcholine	Glutamate	Dopamine	Phenylethylamine
Inhibitor				
	Donepezil	Memantine	Tolcapone	Safinamide

3. Results and Discussion

3.1 Sampling the chemical space

We obtained 1295 tacrine derivatives (see Table S1). However, for 1165 of them, some toxicity values could not be predicted. Consequently, they were removed. The values

of the ADME properties, toxicity, synthetic accessibility, and selection score for all the derivatives and the reference set are given in Tables S2 and Table S3, respectively.

The S^S values of the derivatives range from 0.89 to 1.02. Because of the large amount of the studied molecules, we present only the S^S of the first twenty-five most promising ones (see Figure 1). Our results show that 125 derivatives exhibit a better performance than the parent molecule ($S^S = 0.9$). Nevertheless, only five derivatives (TAC-678, TAC-698, TAC-563, TAC-185, and TAC-674) (see Figure 2) are better scored than the parent molecule and the average value of reference set ($S^S = 1.0$). They are predicted to have all the desirable features of an oral drug (*i.e.*, bioavailability, adequate permeation, low toxicity, and easy manufacturability). Hence, they were chosen for the next stage of the investigation (*i.e.*, the evaluation of their potential as antioxidants).

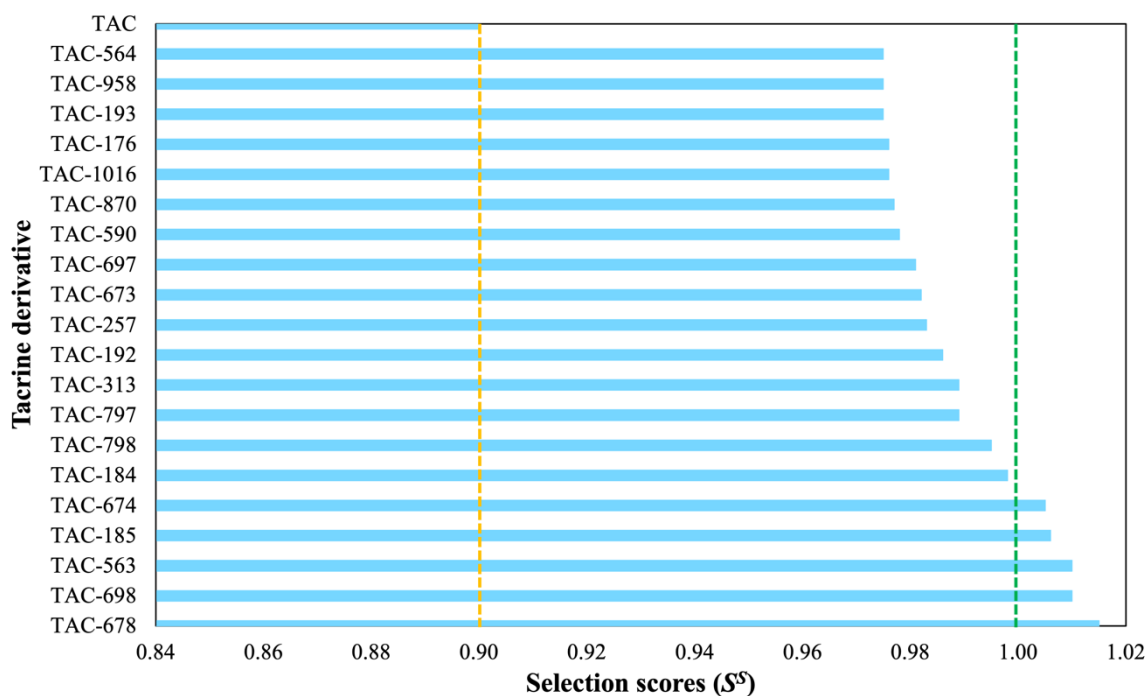


Figure 1. Selection scores S^S of the tacrine derivatives with the best drug-like behavior.

Orange line is the value for tacrine, and green line is the average value of the reference set.

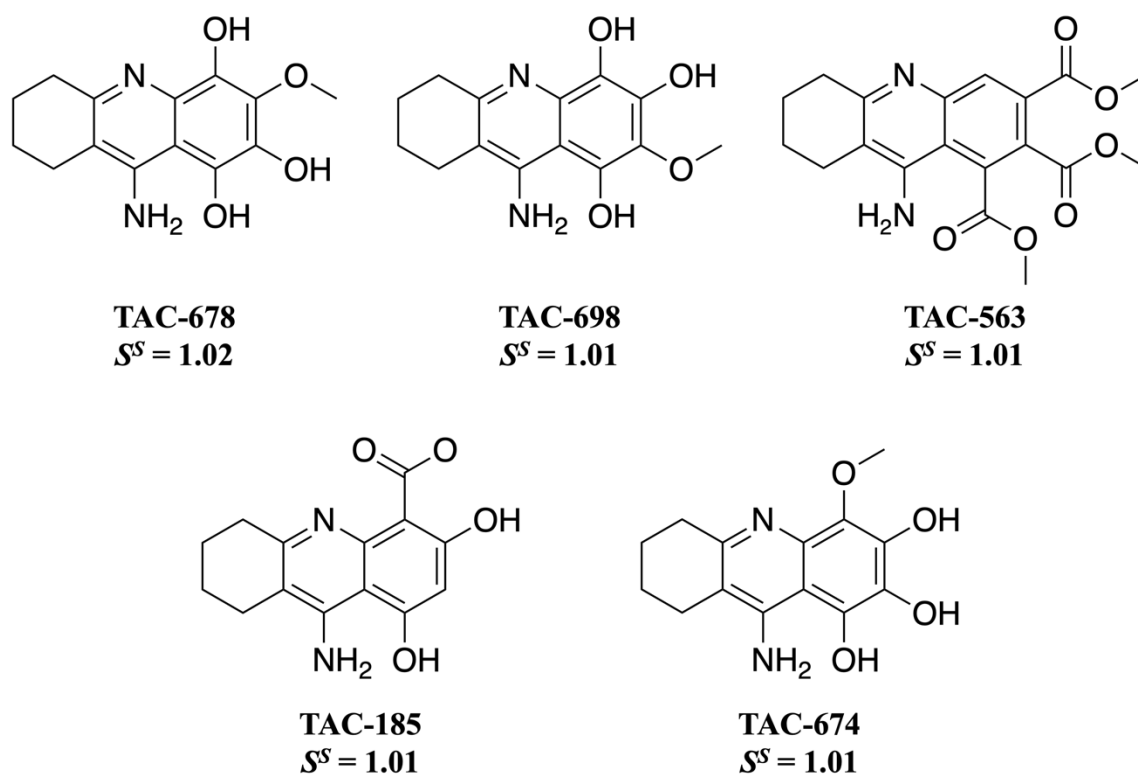


Figure 2. Two-dimensional structures of the best-scored (S^S) tacrine derivatives.

3.2 Acid-base equilibria and antioxidant activity

Unveiling the acid-base equilibria is essential to determine if a molecule can cross a biological barrier through passive diffusion. The pKa values and deprotonation routes are given in Figure S1. Molar fractions in percentage at blood pH are listed in Table 1.

The neutral species of all the selected derivatives are highly abundant at physiological pH. Consequently, all the chosen compounds can easily cross the biological barriers by passive diffusion. However, the cationic forms of TAC-678 and TAC-563 have significant

molar fractions. Besides, the anionic forms of TAC-678 and TAC-698 present non-negligible molar fraction (≥ 1.0 %). Therefore, these anionic species can enhance the antioxidant activity.

IEs and BDEs were computed for the acid-base species with non-negligible molar fractions (*i.e.*, ≥ 1.0 %) (see Table S4). The IEs and the lowest BDE values are given in Table 2. IE and BDE accounts for the capability of a molecule to donate one electron and one H-atom, respectively. Therefore, they were employed to assess the efficacy of tacrine derivatives as free radical scavengers *via* single electron transfer (SET) and hydrogen atom transfer (HAT) mechanisms, respectively. Trolox, ascorbic acid, and tocopherol were used as reference antioxidants. $\text{H}_2\text{O}_2/\bullet\text{OOH}$ pair is the oxidant target. The electron and hydrogen donating ability map for antioxidants (eH-DAMA) is depicted in Figure 3. The anionic forms of TAC-674, TAC-678, and TAC-698 are the most efficient for deactivating hydroperoxyl radicals. They also exhibit a better performance compared with trolox, tocopherol, and ascorbic acid.

Table 2. Estimated pKa and molar fractions (%), $M_{f(q)}$, at pH = 7.4. The q in the acronym corresponds to the charge of the acid-base species.

Derivative	pKa ₁	pKa ₂	pKa ₃	pKa ₄	$M_{f(+1)}$	$M_{f(0)}$	$M_{f(-1)}$	$M_{f(-2)}$	$M_{f(-3)}$
TAC	9.9				99.7	0.3			
TAC-678	7.1	8.8	12.0	17.7	30.0	67.0	3.0	< 0.1	< 0.1
TAC-698	5.7	8.3	12.2	19.4	1.8	87.6	10.5	< 0.1	< 0.1
TAC-563	7.1				31.9	68.1			

TAC-185	4.9	9.9	15.3		0.3	99.3	0.3	< 0.1	
TAC-674	5.1	10.3	11.6	17.2	0.5	99.4	0.1	< 0.1	< 0.1

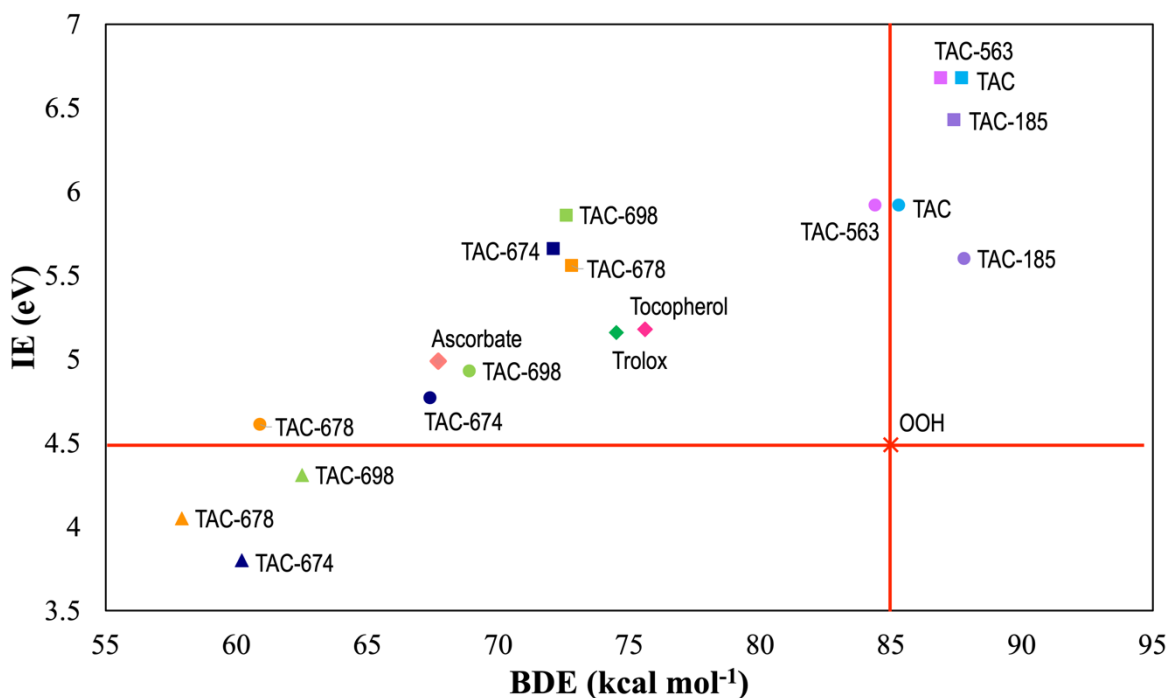


Figure 3. The electron and hydrogen donating ability map (eH-DAMA) of the most promising derivatives and their most abundant acid-base species at physiological pH. Cationic, neutral, and anionic forms are depicted by squares, circles, and triangle figures, respectively.

3.3 Polygenic activity

The potential neuroprotective activity of tacrine derivatives was investigated by molecular docking simulations. The inhibition of key proteins (*i.e.*, AChE, NMDAr, COMT,

and MAO-B) by tacrine derivatives was evaluated calculating the weighted binding energies (ΔG_B^W) and polygenic scores (S^P) (Text S1) and comparing both parameters with the endogenous ligands of these proteins and some reference inhibitors. The ΔG_B^W values of the best derivatives are given in Table 3. The complete docking results are listed in Table S5. Only in the case of MAO-B enzyme, the affinity of the parent molecule is higher compared with the designed compounds. In general, this indicates a marked polygenic behavior. Of note, except for NMDAr, the designed compounds show lower affinity than the reference inhibitors.

Table 3. Weighted binding energies (in kcal mol⁻¹) for TAC and the selected subset of derivatives.

Compound	ΔG_B^W			
	AChE	NMDAr	COMT	MAO-B
TAC	-8.7	-6.6	-5.5	-9.3
TAC-678	-8.7	-7.0	-5.7	-8.9
TAC-698	-8.9	-7.1	-5.5	-9.1
TAC-674	-9.7	-7.0	-6.1	-8.6
Acetylcholine	-4.9			
Glutamate		-5.0		
Dopamine			-5.4	
Phenylethylamine				-6.0
Donepezil	-12.0			

Memantine	-5.8
Tolcapone	-7.6
Safinamide	-10.0

Remarkably, our predicted binding energy for the AChE-tacrine complex ($-8.7 \text{ kcal mol}^{-1}$) aligns closely with experiment ($-8.6 \text{ kcal mol}^{-1}$).⁷⁷ This confirms the reliability of the computational protocol used. Of the derivatives evaluated, TAC-674 exhibits the highest affinity ($-9.7 \text{ kcal mol}^{-1}$) when compared with the parent molecule. This indicates that the rational design applied allowed the identification of derivatives with better theoretical affinity.

A polygenic efficiency plot (see Figure 4) was built to provide a visual assessment of the polypharmacological profile of the designed compounds, based on their binding efficiency relative to the natural substrates (*i.e.*, endogenous ligands). The bar height reflects comparative binding affinity, higher values corresponds to stronger predicted interactions. Notably, the compounds demonstrated the highest predicted inhibitory activity against AChE, NMDAr, and MAO-B.

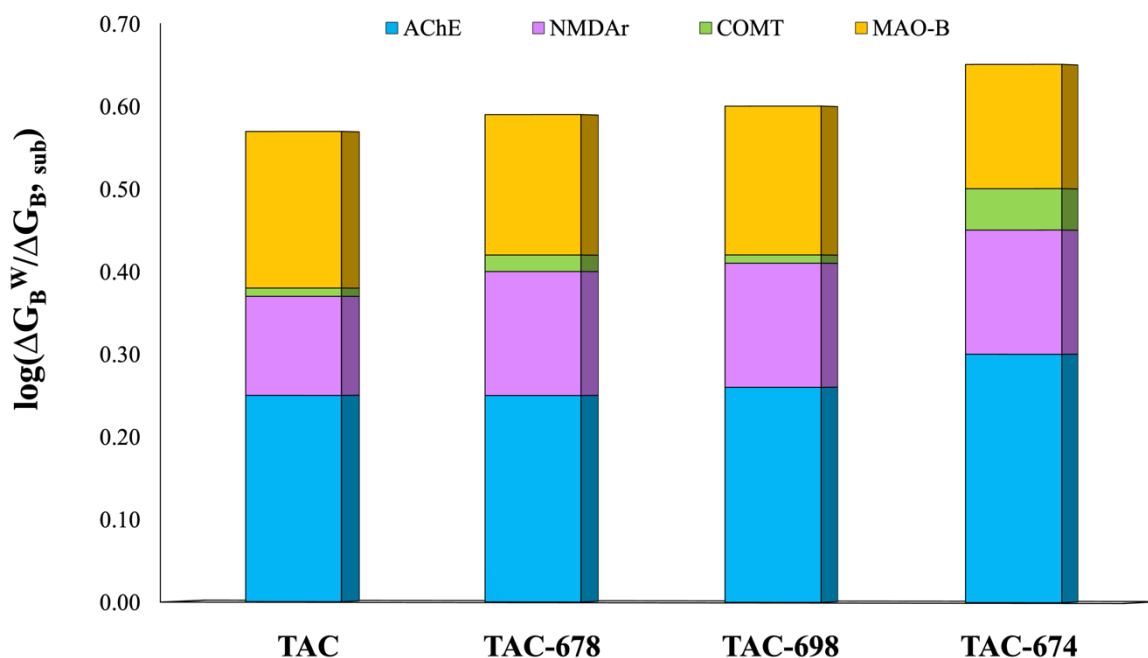


Figure 4. Polygenic scores of tacrine and its derivatives relative to the endogenous ligands.

All the selected derivatives show stronger interactions than the endogenous ligands, being most notable for AChE and NMDAr. The TAC-674 derivative exhibits the most balanced polygenic profile. It maintains high affinity for the main targets (AChE and NMDAr), but also exhibits significant contributions toward COMT and MAO-B. These results support the potential of TAC-674 as a multi-action neuroprotective agent. The plot relative to the reference drugs is presented in the Figure S3. Tacrine and its derivatives show improved affinity only for the NMDA receptor with respect to the reference drugs. In this regard, TAC-698 showed the best affinity against this receptor than memantine, used to treat AD.⁷⁴

In addition to the binding affinities of the protein-ligand complexes, it is essential to consider the conformation of the ligand and the nature of the interactions formed, since these factors contribute to the stability of the complex and provide insights into the possible mechanism of inhibition. To this end, the similarity of interactions score (S_{SI} , Text S1) was used, which allows comparing the pattern of interactions with respect to the natural substrate (NS) or a reference drug (RD). The S_{SI} quantifies the coincidence in the residues involved in the type of interaction (*e.g.*, hydrogen bonds, π interactions, among others) and is expressed as a normalized value between 0 (no similarity) and 1 (complete match). It serves to identify candidates with a similar and functionally relevant binding profile, favoring the rational selection of compounds with potential biological activity comparable to that of reference ligands. Table 4 summarizes the S_{SI} values.

Table 4. Similarity interaction score for the selected tacrine derivatives.

Compound	AChE		NMDAr		COMT		MAO-B	
	NS	RD	NS	RD	NS	RD	NS	RD
TAC	0.14	0.25	0.00	0.62	0.42	0.36	0.36	0.28
TAC-678	0.43	0.50	0.00	0.87	0.00	0.14	0.36	0.50
TAC-698	0.33	0.43	0.00	0.50	0.00	0.14	0.11	0.39
TAC-674	0.36	0.50	0.00	0.50	0.50	0.57	0.49	0.28

$$S_{SI}^{Thr} = 0.36 \text{ (see Text S1)}$$

In general, the highest S_{SI} values were found for the reference drugs and for the NMDA receptor. However, all the chosen derivatives present good S_{SI} values for AChE and MAO-B. TAC-674 and TAC-678 are the derivatives with the most promising interaction profiles, surpassing the threshold on several key targets. TAC-674 stands out for its compatibility with the endogenous ligands and known drugs, reinforcing its multitarget potential and potential balance between efficacy and safety. TAC and TAC-698 have more restricted profiles, with less overall similarity. Our results, suggest that TAC-678 could simultaneously inhibit COMT, MAO-B, NMDAr, and AChE, and exert a multimodal neuroprotective action, with potential applications in neurodegenerative diseases such as AD, PD or even mixed cognitive disorders.

According to the affinity towards the receptors and interaction mode, the most promising compounds to present multi-target function are TAC-678 for MAO-B and NMDAr, and TAC-674 for AChE and COMT, respectively. To unveil the structural origin of these affinities and the potential inhibition mechanisms, it is necessary to analyze the interactions that stabilize the formation of these complexes.

Figure 5 shows the interaction profile of the [MAO-B:TAC-678] complex. TAC-678 forms several stabilized conjugates in the MAO-B active site by interacting with key residues for substrate-specific recognition and inhibitor anchoring in the catalytic environment. Hydrogen bond formation was observed with Tyr326, Gln206, Ile198, Ile199, and Cys172. Tyr326 is known to be critically important as part of the aromatic arc that guides entry into the MAO-B active site.^{76,77} Additionally, hydrophobic interactions with Leu164, Ile316, Leu171, Ile199, and Cys172 as well as additional π -sigma interactions with Leu171 and Ile199 were identified, suggesting efficient anchoring of the aromatic group of TAC-678 in

the hydrophobic cavity. These interactions could increase the permanence of the ligand in the active site, limiting the availability of FAD (Flavin Adenine Dinucleotide) for the oxidation of endogenous amines.^{78,79}

MAO-B is responsible for the catalytic degradation of neuroactive amines such as phenylethylamine and, in part, dopamine. Its inhibition is associated with an increase in the concentration of these neurotransmitters in the neuronal network, which generally results in neuroprotective, antidepressant, and antiparkinsonian effects.⁸⁰ Inhibition of this enzyme has also been proposed as a strategy to reduce the OS-related neurodegeneration.⁸¹ The S_{SI} value of TAC-678 with respect to the reference ligand exceeds the threshold of relevance, suggesting an effective mimetic mechanism of the binding mode of known inhibitors, and therefore, a potential competitive inhibitor.

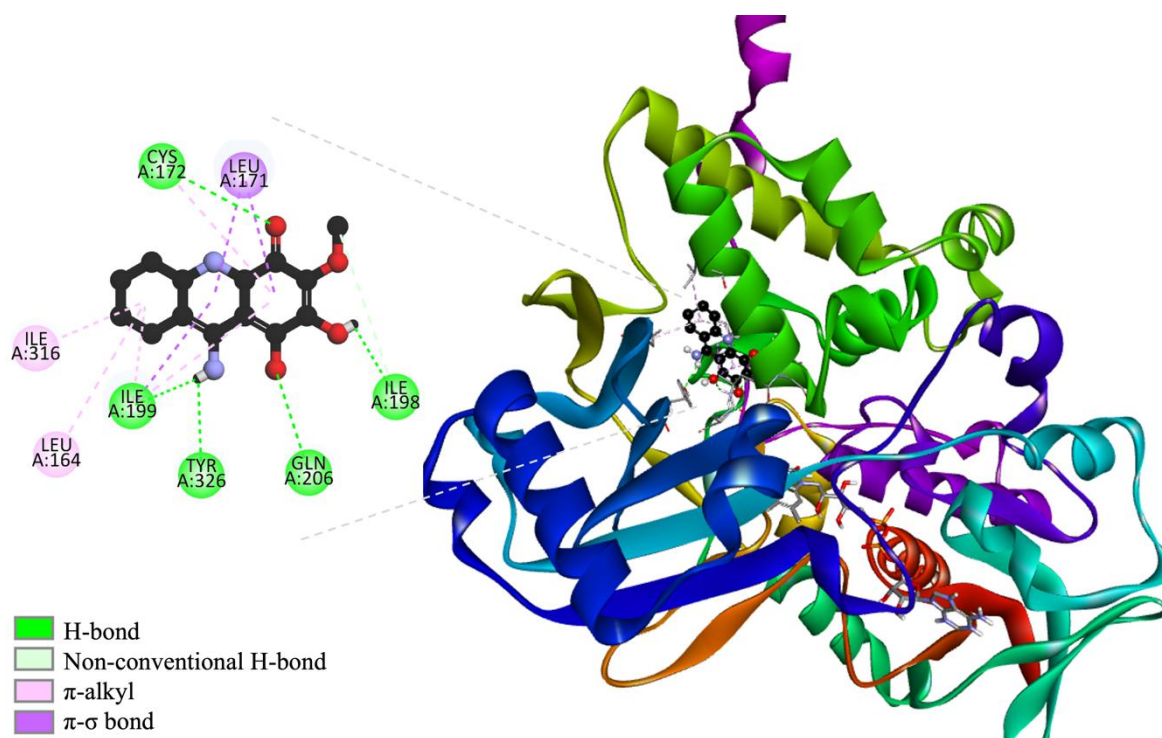


Figure 5. 3D and 2D interaction network in the [MAO-B:TAC-678] complex.

The interactions that stabilize the complex [AChE:TAC-674] are depicted in the Figure 6. TAC-674 exhibits a binding mode that combines specific interactions with residues essential for AChE function. H-bonds are established with Trp86, Asn87, and Tyr124; these amino acids are close to or belong to the active site. In addition, various π -alkyl interactions and π - π stacking were observed with Tyr337, Phe338, and Tyr341, associated with the peripheral site. This region is important in allosteric modulation and ACh scavenging.⁴² This binding mode could imply a dual inhibition mechanism characteristic of potent and multifunctional drugs.^{44,73,82}

The S_{SI} value and the topology of interactions suggest that TAC-674 could act as a mixed or dual AChE inhibitor, disrupting direct catalysis and allosteric regulation. This behavior is desirable in potential drugs against AD, where AChE inhibition is sought to enhance cholinergic signaling.⁸³ Furthermore, peripheral site occupation has been related to a reduction in the formation of A β plaques.⁸⁴

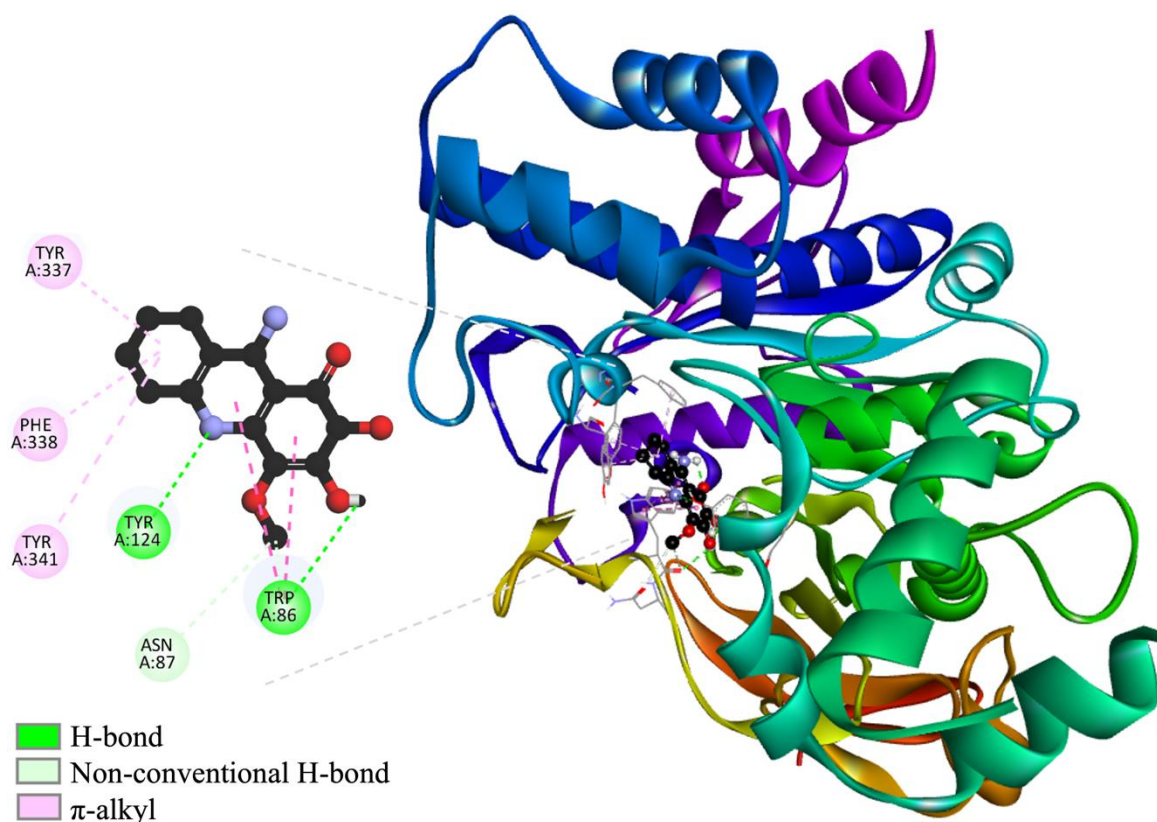


Figure 6. 3D and 2D interaction map in the [AChE:TAC-674] complex.

Figure 7 presents the interactions network that forms the [NMDAr:TAC-678] complex. TAC-678 binds to the NMDA receptor in a region close to the ion channel, with an interaction profile that suggests a functional block similar to that of known antagonists such as memantine or ifenprodil.^{74,85} Ligand binding occurs through various hydrogen bonds with polar residues Asn(B):615, Asn(D):615, and Thr(D):647, suggesting deep insertion, stabilizing the ligand in a position close to the channel. Several non-conventional H-bonds, with Val(B):640, additionally contribute to anchoring, although with lesser strength. Finally, several hydrophobic interactions with Val(D):640, Ala(D):644, and Leu(D):643, reinforce this conformation. Thr(C):648 represents an aesthetic impediment, which could interfere

with the stability or efficacy of the ligand. The ligand arrangement and the variety of chains involved (B, C, D) indicate that TAC-678 is lodged between different subunits of the NMDAr complex, inserting itself into the channel region. This binding pattern resembles the mechanism of action of memantine, which acts as a voltage-gated channel blocker by preventing Ca^{2+} influx without directly competing with orthosteric site ligands.⁸⁶

The S_{SI} values support the idea that the ligand does not mimic glutamate, but rather accurately reproduces interactions of memantine, suggesting that it can act as an antagonist of this protein. The interaction profile suggests that TAC-678 acts as a non-competitive blocker of the NMDA receptor, with the ability to inhibit ion flow in a manner analogous to memantine. This mechanism could be neuroprotective by attenuating excitotoxicity without altering basal physiological neurotransmission.⁸⁷ However, the observed steric hindrance may require structural optimization to improve affinity and reduce conformational strains.

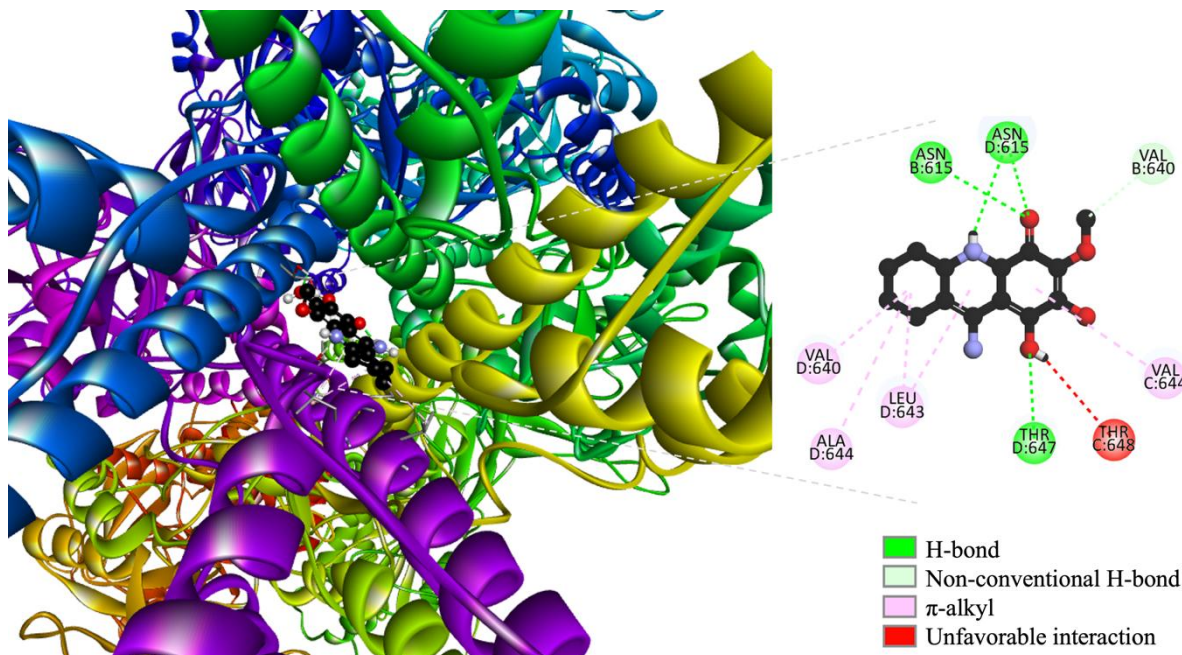


Figure 7. 3D and 2D interaction network in the [NMDAr:TAC678] complex.

Analysis of the binding mode of TAC-674 with COMT enzyme, presented in Figure 8, showed occupancy of this derivative in the catalytic site. A coordination bond is established with the Mg^{2+} ion, an essential cofactor for catechol methylation. This interaction, along with hydrogen bonds with Lys144, Asn170, and Glu199, produces a binding pattern similar to that observed with inhibitors such as tolcapone and entacapone. This binding mode indicates a likely competitive inhibition mechanism.^{88,89} Steric hindrance is also observed with Asn170, which could affect substrate entry dynamics.

Further stabilization of the complex is favored by hydrophobic interactions with Pro174 and Met40, which would reinforce ligand binding in the catalytic cavity. These observations are consistent with the literature on COMT and its inhibitors, where the joint participation of metal-donor bonds, hydrogen bonds and hydrophobic interactions are key for effective inhibition.⁹⁰ The S_{SI} values with the natural substrate and with the reference drug

(0.50 and 0.57) are above the threshold, supporting the pharmacological relevance of TAC-674 as a modulator of catecholamine metabolism in the central nervous system.

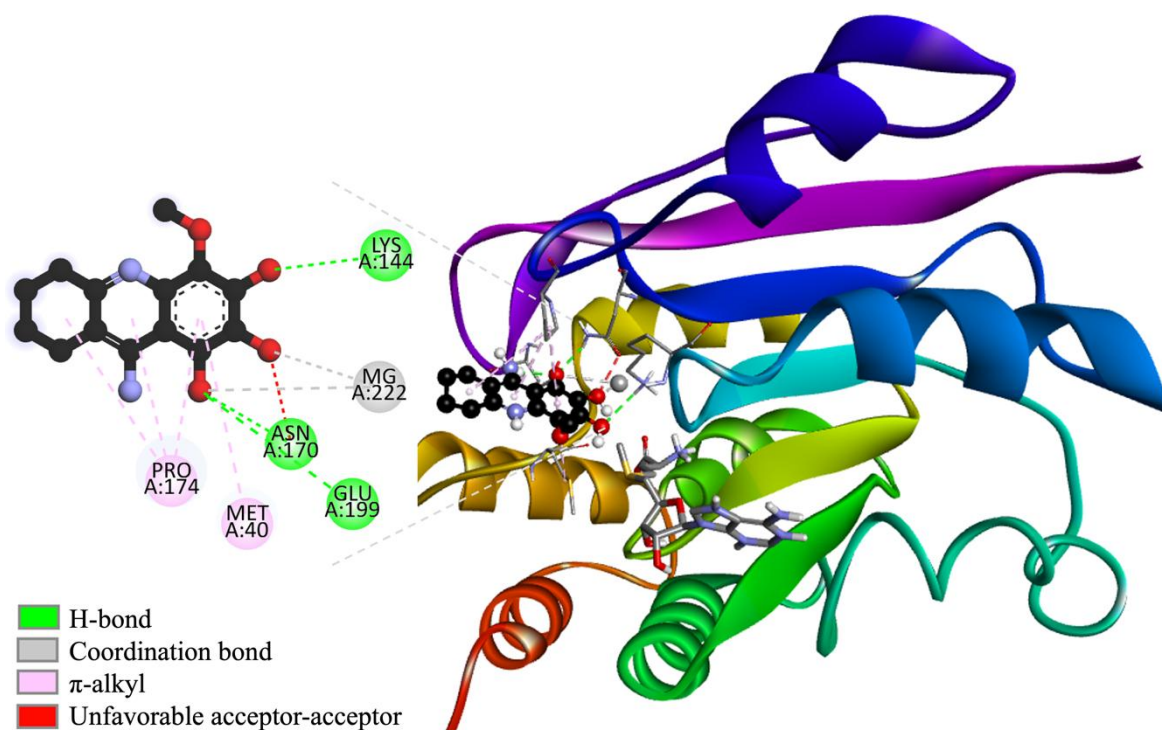


Figure 8. 3D and 2D interaction maps in the [COMT:TAC-674] adduct.

The tacrine analogues analyzed present a potentially neuroprotective action profile, derived from their ability to modulate multiple targets involved in neurodegenerative processes. Their potential inhibition of AChE suggests procognitive effects by increasing synaptic acetylcholine levels. Their interaction with MAO-B and COMT points to an increase in catecholaminergic neurotransmitters, such as dopamine, favoring motor and affective control. Finally, their action on NMDAr, with ion channel blockade, indicates a possible modulatory effect on glutamate excitotoxicity, relevant in pathologies such as AD and PD.

This multi-target profile reinforces their potential as candidates for integrated therapies in complex neurodegenerative diseases.

4. Conclusions

In this work, 1295 tacrine derivatives were designed using the CADMA-Chem methodology. This set was sampled using a selection score based on ADME properties, toxicity, and synthetic accessibility. As a result, we obtained five derivatives with the best drug-like behavior. For this subset, reactivity indexes were calculated to account for H and electron donor capabilities. According to this, TAC-674, TAC-678, and TAC-698 are the best candidates to act as antioxidants. In addition, the docking simulations shown that TAC-674 and TAC-678 are the best inhibitors of AChE and COMT, and MAO-B and NMDAr, respectively.

Acknowledgements

The work in Mexico was supported by project SECIHTI No. CBF2023-2024-1141. We thank the Laboratorio de Visualización y Cómputo Paralelo at Universidad Autónoma Metropolitana Iztapalapa and the HPC Cluster “Kukulcán” at Centro de Investigación y de Estudios Avanzados Mérida for the computing time. E.D. thanks to Estancias Posdoctorales por México (2023) SECIHTI program for the postdoctoral grant. L.F.H.A thanks to Estancias Posdoctorales por México (2022) SECIHTI program for the postdoctoral grant.

References

1. Cacabelos, R. *Int. J. Mol. Sci.* **2025**, 26(15), 7175-7186.
2. Luo, Y.; Qiao, L.; Li, M.; Wen, X.; Zhang, W.; Li, X. *Front. Aging Neurosci.* **2025**, Volume 16 - 2024, 1-12.

3. Thorp, J. G.; Mitchell, B. L.; Gerring, Z. F.; Ong, J.-S.; Gharahkhani, P.; Derks, E. M.; Lupton, M. K. *Neurobiol. Aging* **2022**, *119*, 127-135.
4. Su, D.; Cui, Y.; He, C.; Yin, P.; Bai, R.; Zhu, J.; Lam, J. S. T.; Zhang, J.; Yan, R.; Zheng, X.; Wu, J.; Zhao, D.; Wang, A.; Zhou, M.; Feng, T. *BMJ* **2025**, *388*, e080952.
5. García-Morales, V.; González-Acedo, A.; Melguizo-Rodríguez, L.; Pardo-Moreno, T.; Costela-Ruiz, V. J.; Montiel-Troya, M.; Ramos-Rodríguez, J. J. *Biomedicines* **2021**, *9*(12), 1910.
6. Zhang, J.; Zhang, Y.; Wang, J.; Xia, Y.; Zhang, J.; Chen, L. *Signal Transduction Targeted Ther.* **2024**, *9*(1), 211.
7. Vecchio, I.; Sorrentino, L.; Paoletti, A.; Marra, R.; Arbitrio, M. *J. Cent. Nerv. Syst. Dis.* **2021**, *13*, 11795735211029113.
8. He, J.; Tam, K. Y. *Drug. Discov. Today* **2024**, *29*(4), 103914.
9. Uddin, M. S.; Al Mamun, A.; Kabir, M. T.; Ashraf, G. M.; Bin-Jumah, M. N.; Abdel-Daim, M. M. *Mol. Neurobiol.* **2021**, *58*(1), 281-303.
10. Zhang, F.; Zhong, R. J.; Cheng, C.; Li, S.; Le, W. D. *Acta Pharmacol. Sin.* **2021**, *42*(9), 1382-1389.
11. Chopade, P.; Chopade, N.; Zhao, Z.; Mitragotri, S.; Liao, R.; Chandran Suja, V. *Bioeng. Transl. Med.* **2023**, *8*(1), e10367.
12. Behl, T.; Makkar, R.; Sehgal, A.; Singh, S.; Sharma, N.; Zengin, G.; Bungau, S.; Andronie-Cioara, F. L.; Munteanu, M. A.; Brisc, M. C.; Uivarosan, D.; Brisc, C. *Int. J. Mol. Sci.* **2021**, *22*(14).
13. Dhapola, R.; Beura, S. K.; Sharma, P.; Singh, S. K.; HariKrishnaReddy, D. *Mol. Biol. Rep.* **2024**, *51*(1), 48.

14. Ali, J.; Choe, K.; Park, J. S.; Park, H. Y.; Kang, H.; Park, T. J.; Kim, M. O. *Antioxidants* **2024**, *13*(7), 862.
15. Asim, A.; Jastrzębski, M. K.; Kaczor, A. A. *Molecules* **2025**, *30*(14), 2975.
16. Cruz-Vicente, P.; Passarinha, L. A.; Silvestre, S.; Gallardo, E. *Molecules* **2021**, *26*(8), 2193-2221.
17. Srinivasan, E.; Chandrasekhar, G.; Chandrasekar, P.; Anbarasu, K.; Vickram, A. S.; Karunakaran, R.; Rajasekaran, R.; Srikumar, P. S. *Front. Med.* **2021**, *Volume 8* - 2021.
18. Yi, S.; Wang, L.; Wang, H.; Ho, M. S.; Zhang, S. *Int. J. Mol. Sci.* **2022**, *23*(23), 14753.
19. Zhou, Z. D.; Yi, L. X.; Wang, D. Q.; Lim, T. M.; Tan, E. K. *Transl. Neurodegener.* **2023**, *12*(1), 44.
20. Juárez Olguín, H.; Calderón Guzmán, D.; Hernández García, E.; Barragán Mejía, G. *Oxid. Med. Cell. Longev.* **2016**, *2016*, 9730467.
21. Speranza, L.; Di Porzio, U.; Viggiano, D.; de Donato, A.; Volpicelli, F. *Cells* **2021**, *10*(4), 735.
22. Kang, S. S.; Ahn, E. H.; Zhang, Z.; Liu, X.; Manfredsson, F. P.; Sandoval, I. M.; Dhakal, S.; Iuvone, P. M.; Cao, X.; Ye, K. *Embo J.* **2018**, *37*(12).
23. Baweja, G. S.; Gupta, S.; Kumar, B.; Patel, P.; Asati, V. *Mol. Divers.* **2024**, *28*(3), 1823-1845.
24. Sequeira, L.; Benfeito, S.; Fernandes, C.; Lima, I.; Peixoto, J.; Alves, C.; Machado, C. S.; Gaspar, A.; Borges, F.; Chavarria, D. *Pharmaceutics* **2024**, *16*(6), 708.
25. Wang, H.; Pan, J.; Zhang, M.; Tan, Z. *Front. Pharmacol.* **2025**, *Volume 16* - 2025.
26. Dong-Chen, X.; Yong, C.; Yang, X.; Chen-Yu, S.; Li-Hua, P. *Signal. Transduct. Target. Ther.* **2023**, *8*(1), 73.

27. Regensburger, M.; Ip, C. W.; Kohl, Z.; Schrader, C.; Urban, P. P.; Kassubek, J.; Jost, W. H. *J. Neural. Transm. (Vienna)* **2023**, *130*(6), 847-861.
28. Stocchi, F.; Bravi, D.; Emmi, A.; Antonini, A. *Nat. Rev. Neurol.* **2024**, *20*(12), 695-707.
29. Cohen, J.; Mathew, A.; Dourvetakis, K. D.; Sanchez-Guerrero, E.; Pangen, R. P.; Gurusamy, N.; Aenlle, K. K.; Ravindran, G.; Twahir, A.; Isler, D. *Cells* **2024**, *13*(6), 511.
30. Eckroat, T. J.; Manross, D. L.; Cowan, S. C. *Int. J. Mol. Sci.* **2020**, *21*(17), 5965.
31. Bautista-Aguilera, Ó. M.; Ismaili, L.; Iriepa, I.; Diez-Iriepa, D.; Chabchoub, F.; Marco-Contelles, J.; Pérez, M. *Chem. Rec.* **2021**, *21*(1), 162-174.
32. Mitra, S.; Muni, M.; Shawon, N. J.; Das, R.; Emran, T. B.; Sharma, R.; Chandran, D.; Islam, F.; Hossain, M. J.; Safi, S. Z.; Sweilam, S. H. *Oxid. Med. Cell. Longev.* **2022**, *2022*, 7252882.
33. Dogga, B.; Reddy, E. K.; Sharanya, C. S.; Abhithaj, J.; Arun, K. G.; Ananda Kumar, C. S.; Rangappa, K. S. *Eur. J. Med. Chem. Rep.* **2022**, *6*, 100094.
34. Buble, A.; Erofeev, A.; Gorelkin, P.; Beloglazkina, E.; Majouga, A.; Krasnovskaya, O. *Int. J. Mol. Sci.* **2023**, *24*(2), 1717-1770.
35. Fares, S.; El Husseiny, W. M.; Selim, K. B.; Massoud, M. A. M. *ACS Omega* **2023**, *8*(29), 26012-26034.
36. Marucci, G.; Buccioni, M.; Ben, D. D.; Lambertucci, C.; Volpini, R.; Amenta, F. *Neuropharmacology* **2021**, *190*, 108352.
37. Mak, S.; Li, W.; Fu, H.; Luo, J.; Cui, W.; Hu, S.; Pang, Y.; Carlier, P. R.; Tsim, K. W.; Pi, R.; Han, Y. *J. Neurochem.* **2021**, *158*(6), 1381-1393.
38. Guzmán-López, E. G.; Reina, M.; Hernández-Ayala, L. F.; Galano, A. *Antioxidants* **2023**, *12*(6), 1256.

39. Guzman-Lopez, E. G.; Reina, M.; Perez-Gonzalez, A.; Francisco-Marquez, M.; Hernandez-Ayala, L. F.; Castañeda-Arriaga, R.; Galano, A. *Int. J. Mol. Sci.* **2022**, *23*(21), 13246-13272.
40. Reina, M.; Guzmán-López, E. G.; Galano, A. *Int. J. Quantum Chem.* **2023**, *123*(2), e27011.
41. Pérez-González, A.; Castañeda-Arriaga, R.; Guzmán-López, E. G.; Hernández-Ayala, L. F.; Galano, A. *ACS omega* **2022**, *7*(43), 38254-38268.
42. Hernández-Ayala, L. F.; Guzmán-López, E. G.; Galano, A. *Antioxidants* **2023**, *12*(10), 1853.
43. Morales-Garcia, B.; Pérez-González, A.; Álvarez-Idaboy, J. R.; Galano, A. *J. Mol. Model.* **2025**, *31*(1), 1-14.
44. Prejanò, M.; Romeo, I.; Felipe Hernández-Ayala, L.; Gabriel Guzmán-López, E.; Alcaro, S.; Galano, A.; Marino, T. *ChemPhysChem* **2025**, *26*(1), e202400653.
45. Guzman-Lopez, E. G.; Galano, A.: CDMX, 2024.
46. Guzman-Lopez, E. G.; Galano, A.: CDMX, 2024.
47. Lipinski, C. A.; Lombardo, F.; Dominy, B. W.; Feeney, P. J. *Adv. Drug Delivery Rev.* **1997**, *23*(1-3), 3-25.
48. Ghose, A. K.; Viswanadhan, V. N.; Wendoloski, J. J. *J. Comb. Chem.* **1999**, *1*(1), 55-68.
49. Egan, W. J.; Merz, K. M.; Baldwin, J. J. *J. Med. Chem.* **2000**, *43*(21), 3867-3877.
50. Muegge, I.; Heald, S. L.; Brittelli, D. *J. Med. Chem.* **2001**, *44*(12), 1841-1846.
51. Veber, D. F.; Johnson, S. R.; Cheng, H.-Y.; Smith, B. R.; Ward, K. W.; Kopple, K. *D. J. Med. Chem.* **2002**, *45*(12), 2615-2623.
52. Martin, T.; U.S Environmental Protection Agency: Cincinnati, Ohio, 2020.

53. Kochev, N.; Avramova, S.; Angelov, P.; Jeliaskova, N. *Org. Chem. Ind. J* **2018**, *14*(2), 123.
54. Zhao, Y.; Schultz, N. E.; Truhlar, D. G. *J. Chem. Theory Comput.* **2006**, *2*(2), 364-382.
55. Galano, A.; Alvarez-Idaboy, J. R. *J. Comput. Chem.* **2014**, *35*(28), 2019-2026.
56. Galano, A. *J. Mex. Chem. Soc.* **2015**, *59*(4), 231-262.
57. Zhao, Y.; Truhlar, D. G. *J. Phys. Chem. A* **2008**, *112*(6), 1095-1099.
58. Galano, A.; Pérez-González, A.; Castañeda-Arriaga, R.; Muñoz-Rugeles, L.; Mendoza-Sarmiento, G.; Romero-Silva, A.; Ibarra-Escutia, A.; Rebollar-Zepeda, A. M.; León-Carmona, J. R.; Hernández-Olivares, M. A. *J. Chem. Inf. Model.* **2016**, *56*(9), 1714-1724.
59. Rebollar-Zepeda, A. M.; Galano, A. *Int. J. Quantum Chem.* **2012**, *112*(21), 3449-3460.
60. Pérez-González, A.; Castañeda-Arriaga, R.; Verastegui, B.; Carreón-González, M.; Alvarez-Idaboy, J. R.; Galano, A. *Theor. Chem. Acc.* **2018**, *137*, 1-10.
61. Marenich, A. V.; Cramer, C. J.; Truhlar, D. G. *J. Phys. Chem. B* **2009**, *113*(18), 6378-6396.
62. Frisch, M. J.; Trucks, G. W.; Schlegel, H. B.; Scuseria, G. E.; Robb, M. A.; Cheeseman, J. R.; Scalmani, G.; Barone, V.; Mennucci, B.; Petersson, G. A.; Nakatsuji, H.; Caricato, M.; Li, X.; Hratchian, H. P.; Izmaylov, A. F.; Bloino, J.; Zheng, G.; Sonnenberg, J. L.; Hada, M.; Ehara, M.; Toyota, K.; Fukuda, R.; Hasegawa, J.; Ishida, M.; Nakajima, T.; Honda, Y.; Kitao, O.; Nakai, H.; Vreven, T.; Montgomery, J., J. A. ; Peralta, J. E.; Ogliaro, F.; Bearpark, M.; Heyd, J. J.; Brothers, E.; Kudin, K. N.; Staroverov, V. N.; Keith, T.; Kobayashi, R.; Normand, J.; Raghavachari, K.; Rendell, A.; Burant, J. C.; Iyengar, S. S.;

Tomasi, J.; Cossi, M.; Rega, N.; Millam, J. M.; Klene, M.; Knox, J. E.; Cross, J. B.; Bakken, V.; Adamo, C.; Jaramillo, J.; Gomperts, R.; Stratmann, R. E.; Yazyev, O.; Austin, A. J.; Cammi, R.; Pomelli, C.; Ochterski, J. W.; Martin, R. L.; Morokuma, K.; Zakrzewski, V. G.; Voth, G. A.; Salvador, P.; Dannenberg, J. J.; Dapprich, S.; Daniels, A. D.; Farkas, O.; Foresman, J. B.; Ortiz, J. V.; Cioslowski, J.; Fox, D. J.; Gaussian Inc.: Wallingford, CT, 2013.

63. Dzib, E.; Cabellos, J. L.; Ortíz-Chi, F.; Pan, S.; Galano, A.; Merino, G. *Int. J. Quantum Chem.* **2019**, *119*(2), e25686.

64. ; Chemaxon: Budapest, 2024.

65. Berman, H. M.; Westbrook, J.; Feng, Z.; Gilliland, G.; Bhat, T. N.; Weissig, H.; Shindyalov, I. N.; Bourne, P. E. *Nucleic Acids Res.* **2000**, *28*(1), 235-242.

66. Webb, B.; Sali, A. *Curr. Protoc. Bioinf.* **2016**, *54*(1), 5.6.1-5.6. 37.

67. Schwede, T.; Kopp, J.; Guex, N.; Peitsch, M. C. *Nucleic Acids Res.* **2003**, *31*(13), 3381-3385.

68. Morris, G. M.; Huey, R.; Lindstrom, W.; Sanner, M. F.; Belew, R. K.; Goodsell, D. S.; Olson, A. J. *J. Comput. Chem.* **2009**, *30*(16), 2785-2791.

69. Eberhardt, J.; Santos-Martins, D.; Tillack, A. F.; Forli, S. *J. Chem. Inf. Model.* **2021**, *61*(8), 3891-3898.

70. Trott, O.; Olson, A. J. *J. Comput. Chem.* **2010**, *31*(2), 455-461.

71. BIOVIA, D. S.; Dassault Systèmes: San Diego, 2025.

72. Pettersen, E. F.; Goddard, T. D.; Huang, C. C.; Couch, G. S.; Greenblatt, D. M.; Meng, E. C.; Ferrin, T. E. *J. Comput. Chem.* **2004**, *25*(13), 1605-1612.

73. Cheung, J.; Rudolph, M. J.; Burshteyn, F.; Cassidy, M. S.; Gary, E. N.; Love, J.; Franklin, M. C.; Height, J. J. *J. Med. Chem.* **2012**, *55*(22), 10282-10286.

74. Chou, T.-H.; Epstein, M.; Michalski, K.; Fine, E.; Biggin, P. C.; Furukawa, H. *Nat. Struct. Mol. Biol.* **2022**, 29(6), 507-518.
75. Ellermann, M.; Lerner, C.; Burgy, G.; Ehler, A.; Bissantz, C.; Jakob-Roetne, R.; Paulini, R.; Allemann, O.; Tissot, H.; Grünstein, D. *Biol. Crystallogr.* **2012**, 68(3), 253-260.
76. Binda, C.; Wang, J.; Pisani, L.; Caccia, C.; Carotti, A.; Salvati, P.; Edmondson, D. E.; Mattevi, A. *J. Med. Chem.* **2007**, 50(23), 5848-5852.
77. Binda, C.; Aldeco, M.; Geldenhuys, W. J.; Tortorici, M.; Mattevi, A.; Edmondson, D. E. *ACS Med. Chem. Lett.* **2012**, 3(1), 39-42.
78. Son, S. Y.; Ma, J.; Kondou, Y.; Yoshimura, M.; Yamashita, E.; Tsukihara, T. *Proc. Natl. Acad. Sci. U S A* **2008**, 105(15), 5739-5744.
79. Youdim, M. B.; Edmondson, D.; Tipton, K. F. *Nat. Rev. Neurosci.* **2006**, 7(4), 295-309.
80. Finberg, J. P. *Pharmacol. Ther.* **2014**, 143(2), 133-152.
81. Carradori, S.; Gidaro, M. C.; Petzer, A.; Costa, G.; Guglielmi, P.; Chimenti, P.; Alcaro, S.; Petzer, J. P. *J. Agric. Food. Chem.* **2016**, 64(47), 9004-9011.
82. Harel, M.; Schalk, I.; Ehret-Sabatier, L.; Bouet, F.; Goeldner, M.; Hirth, C.; Axelsen, P.; Silman, I.; Sussman, J. *PNAS* **1993**, 90(19), 9031-9035.
83. Colović, M. B.; Krstić, D. Z.; Lazarević-Pašti, T. D.; Bondžić, A. M.; Vasić, V. M. *Curr. Neuropharmacol.* **2013**, 11(3), 315-335.
84. Inestrosa, N. C.; Alvarez, A.; Pérez, C. A.; Moreno, R. D.; Vicente, M.; Linker, C.; Casanueva, O. I.; Soto, C.; Garrido, J. *Neuron* **1996**, 16(4), 881-891.
85. Tajima, N.; Karakas, E.; Grant, T.; Simorowski, N.; Diaz-Avalos, R.; Grigorieff, N.; Furukawa, H. *Nature* **2016**, 534(7605), 63-68.
86. Lipton, S. A.; Chen, H. S. *Expert. Opin. Ther. Targets* **2005**, 9(3), 427-429.

87. Parsons, C. G.; Stöffler, A.; Danysz, W. *Neuropharmacology* **2007**, *53*(6), 699-723.
88. Männistö, P. T.; Keränen, T.; Reinikainen, K. J.; Hanttu, A.; Pollesello, P. *Neurol. Ther.* **2024**, *13*(4), 1039-1054.
89. Bonifácio, M. J.; Palma, P. N.; Almeida, L.; Soares-da-Silva, P. *CNS Drug Rev.* **2007**, *13*(3), 352-379.
90. Männistö, P. T.; Kaakkola, S. *Pharmacol. Rev.* **1999**, *51*(4), 593-628.